

# Dibenzothienobisbenzothiophene—a novel fused-ring oligomer with high field-effect mobility

Henning Sirringhaus,<sup>\*a</sup> Richard H. Friend,<sup>a</sup> Changsheng Wang,<sup>b†</sup> Jörg Leuninger<sup>b</sup> and Klaus Müllen<sup>b</sup>

<sup>a</sup>*Cavendish Laboratory, University of Cambridge, Madingley Road, Cambridge, UK CB3 0HE.*

*E-mail: hs220@phy.cam.ac.uk*

<sup>b</sup>*Max-Planck-Institut für Polymerforschung, Ackermannweg 10, 55128 Mainz, FRG*

Received 6th April 1999, Accepted 12th May 1999

Conjugated oligomers with rigid, fused-ring structure are of interest for organic field-effect transistors where strong  $\pi$ - $\pi$  interaction between adjacent molecules is required to obtain high charge carrier mobilities. Dibenzo[*b,b'*]thieno[2,3-*f'*:5,4-*f''*]bis[1]benzothiophene (DBTBT) has been synthesized by a novel route, the key step of which is the acid-induced intramolecular cyclization reaction of aromatic methyl sulfoxides. Field-effect transistors (FETs) with thin, polycrystalline DBTBT films deposited by vacuum sublimation exhibit high field-effect mobilities of  $0.15 \text{ cm}^2 (\text{Vs})^{-1}$  and ON-OFF current ratios  $> 10^6$ . The coupling reaction is not regioselective and different regioisomers have been identified. Degraded FET performance is observed when the sublimed films contain a mixture of different isomers.

## 1. Introduction

Electronic devices based on conjugated organic semiconductors such as field-effect transistors (FETs) have recently attracted renewed attention. Potential applications of organic FETs encompass cheap logic circuits on plastic substrates for use in identification tags and memory elements<sup>1</sup> as well as integrated optoelectronic devices, such as pixel drive and switching elements in active-matrix organic light-emitting diode (LED) displays.<sup>2</sup> The simplest and most common device configuration is that of a thin-film transistor, in which a thin film of the organic semiconductor is deposited on top of a dielectric with an underlying gate electrode. Charge-injecting source-drain (S-D) contacts providing ohmic contacts are defined either on top of the organic film ('top-contact' configuration) or on the surface of the FET substrate prior to the deposition of the semiconductor ('bottom-contact' configuration). Most organic FETs operate in p-type accumulation mode.<sup>3</sup> When a negative voltage is applied to the gate, holes are injected from the S-D contacts into a thin accumulation layer at the interface between the semiconductor and the gate dielectric. The S-D current is determined by the conductivity of this thin sheet of field-induced charges at the interface and should increase rapidly with gate voltage. In order to obtain low OFF-currents and high ON-OFF current ratios  $> 10^6$  the bulk of the semiconductor should have low conductivity and low extrinsic doping concentration.

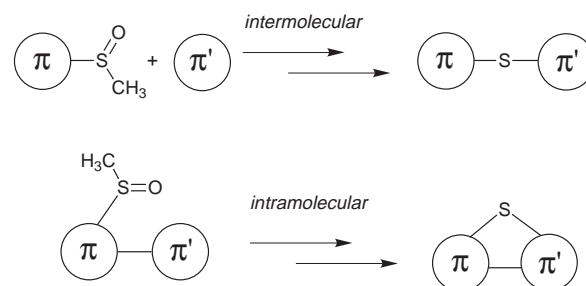
For most practical applications the mobility of the field-induced charges needs to be  $> 0.1\text{--}1 \text{ cm}^2 (\text{Vs})^{-1}$ . Initiated by the pioneering work on oligothiophenes (*n-T*)<sup>4</sup> such high mobility values have recently been demonstrated for various conjugated oligomers<sup>5-7</sup> and polymers.<sup>2</sup> Highly-ordered polycrystalline films of conjugated oligomers can be deposited by vacuum sublimation. In most thiophene and acene oligomer FETs the molecules are preferentially oriented with their long axis close to normal to the FET substrate. Efficient charge transport in the plane of the film can occur along the direction of intermolecular  $\pi$ - $\pi$  stacking. One of the important questions is how the intramolecular structure is related to the strength of the intermolecular  $\pi$ - $\pi$  interactions and the charge carrier

mobility. Of particular interest are ladder-type, fused-ring compounds.<sup>5,8</sup> It has been suggested that fused-ring bisdithienothiophene exhibits a higher mobility than the corresponding 4-T oligothiophene, as a result of pronounced coplanar  $\pi$ - $\pi$  stacking.<sup>9</sup> To date the highest FET mobilities of  $1\text{--}3 \text{ cm}^2 \text{ V}^{-1} \text{ s}^{-1}$  have been reported for pentacene.<sup>7</sup> However, the synthesis of fused-ring compounds is often difficult, and only a few materials have been investigated. Here we present the synthesis and field-effect mobility of a new fused-ring compound, dibenzo[*b,b'*]thieno[2,3-*f'*:5,4-*f''*]bis[1]benzothiophene (DBTBT, **1**).

## 2. Synthesis

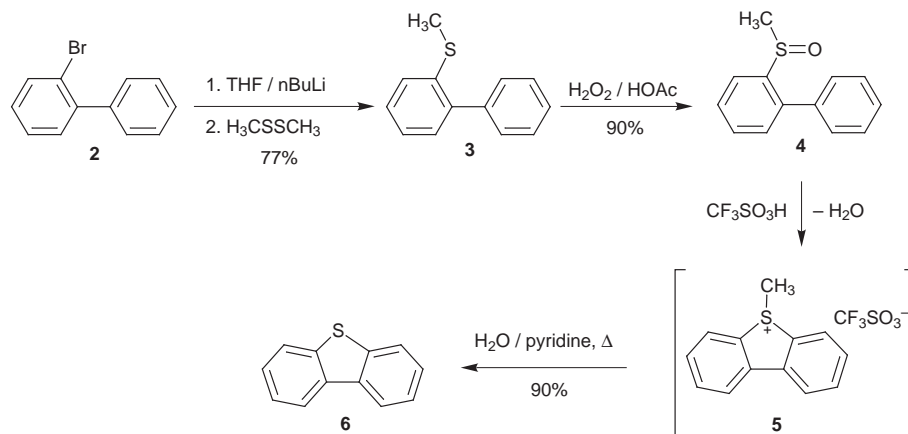
For the synthesis of DBTBT, **1** we developed a unique synthetic approach. The key step of this method is the coupling reaction of aromatic methyl sulfoxides with activated aromatic building blocks in the presence of strong acids. This type of reaction has already been used in an *intermolecular* fashion for the preparation of high-molecular weight polymers, such as poly(phenylene sulfide) (PPS),<sup>10,11</sup> poly(phenylene sulfide-phenyleneamine) (PPSA)<sup>12,13</sup> and poly(phenylene sulfidephenyleneamine-phenyleneamine)(PPSAA).<sup>14</sup> However, to the best of our knowledge, the *intramolecular*, acid-induced condensation under formation of dibenzothiophene-based systems has not been described yet (Scheme 1).

In preliminary studies, we investigated the suitability of this type of reaction on the level of a model system (Scheme 2). Methylsulfinylbiphenyl (**4**) was synthesized in two steps



**Scheme 1** Concepts for the inter- and intramolecular acid-induced coupling reaction of aromatic methyl sulfoxides.

<sup>†</sup> *Current address:* Department of Chemistry, University of Durham, Durham UK DH1 3LE.



**Scheme 2** Synthesis of dibenzothiophene (**6**) as a model system for the intramolecular acid-induced cyclization reaction of 2-(methylsulfonyl)bi-phenyl (**4**).

according to Scheme 2 and treated with the strong trifluoromethanesulfonic acid. The intermediate sulfonium salt **5** was not isolated and subsequent demethylation with a water-pyridine mixture (5:1) afforded the dibenzothiophene (**6**) in 90% yield.

The success of this novel type of dibenzothiophene formation raised the question, how to construct a useful precursor molecule for DBTBT **1**. Two structures seemed possible (Scheme 3). However, compound **7** is not the molecule of choice, as the first cyclization step yields a sulfonium salt, which deactivates the entire molecule towards a second or even third attack at the remaining sulfoxides. Therefore, precursor **8** is favorable, as it already contains one dibenzothiophene unit, which in the coupling reaction might act as an activating group. Hence, the target structure on the way towards the synthesis of DBTBT **1** is the 3,7-bis(2-methylsulfinylphenyl)dibenzothiophene (**8**).

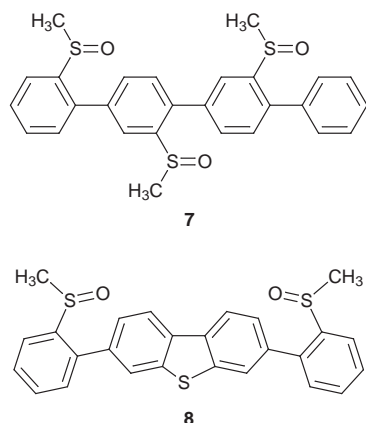
The synthetic route to **8** is described in Scheme 4. Starting from the commercially available dibenzothiophene (**9**), dibenzothiophene dioxide (**10**) is obtained quantitatively by oxidation in glacial acetic acid with hydrogen peroxide according to the literature.<sup>15</sup> In contrast to the tedious known procedure,<sup>16</sup> **10** is dibrominated with dibromocyanuric acid<sup>17</sup> in one step to afford 3,7-dibromodibenzothiophene dioxide (**11**). Reduction with lithium aluminium hydride yields the 3,7-dibromodibenzothiophene (**12**) in 59% yield.<sup>18</sup> Dilithiation of **12**, subsequent reaction with triisopropyl borate followed by hydrolysis give dibenzothiophene-3,7-diboronic acid (**13**) along with a not separable byproduct, the 3-bromodibenzothiophene-7-boronic acid (**14**). The final step towards the precursor **8** includes an aryl-aryl-type coupling reaction according to Suzuki<sup>19</sup> of the mixture of **13** and **14** with 2-bromo(methyl-

sulfonyl)benzene (**16**). **16** can be obtained in high yields by oxidation of 2-bromo(methylsulfonyl)benzene (**15**) in glacial acetic acid with hydrogen peroxide. The precursor **8** can be isolated along with a second product, which was identified by mass spectrometry and NMR spectroscopy as **17**. The formation of this byproduct can be explained by the presence of the monobromo derivative **14** in the mixture of the starting materials and is described in Scheme 5. However, at this stage of the synthesis **8** and **17** can be separated by column chromatography and the target structure, precursor **8** can be obtained in 51% yield.

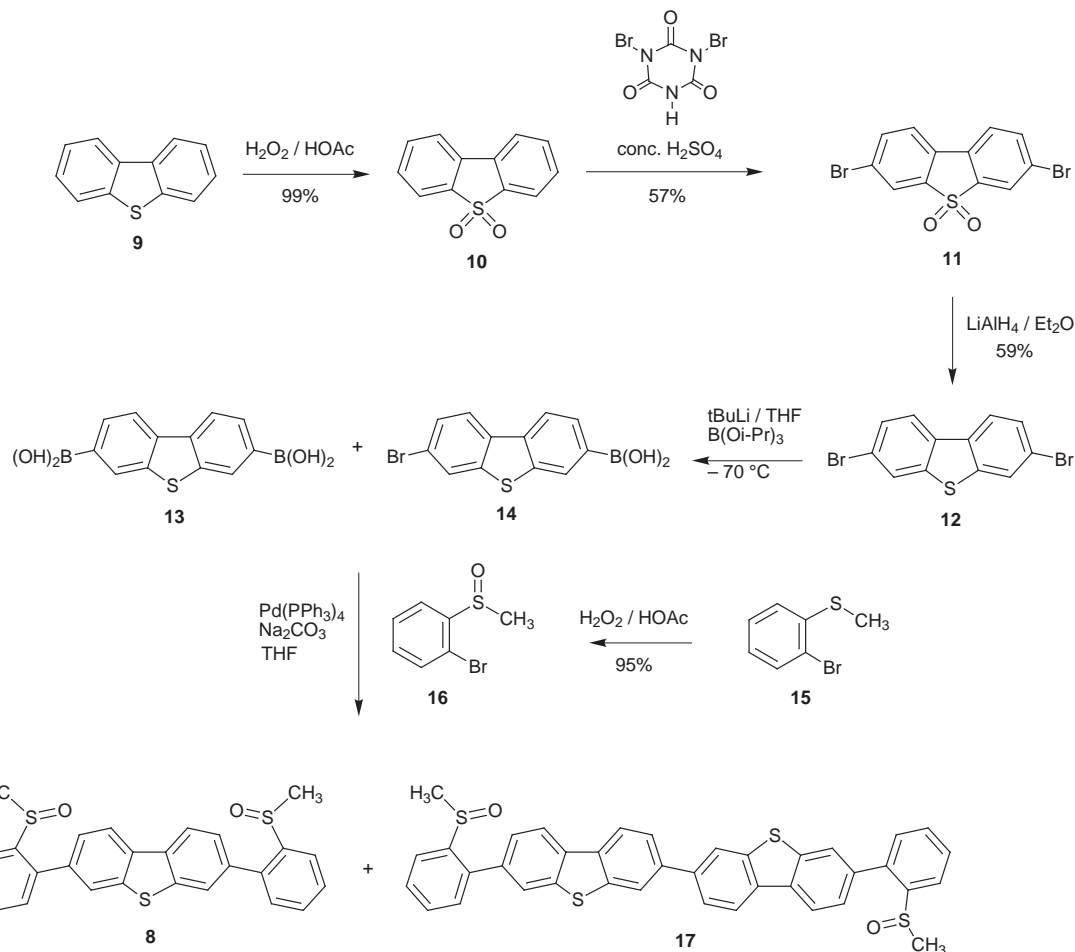
The final step towards the synthesis of DBTBT **1** is performed by treating **8** with trifluoromethanesulfonic acid for 12 h (Scheme 6). A yellow solid is obtained after hydrolysis, which is insoluble in ordinary organic solvents. Further characterization was not performed and the structure was assumed to be **18**. The final demethylation is achieved by refluxing the solid in pyridine for 12 h. DBTBT **1** is obtained after hydrolysis and crystallisation from boiling quinoline as pale yellow plates in 86% yield (related to the starting material **8**).

The solid has a modest solubility in dichlorobenzene at room temperature, which allowed the determination of a UV-VIS spectrum with three absorption maxima at 374, 394 and 415 nm. However, the solubility of this compound is not sufficient for NMR spectroscopy. FD-mass spectrometry revealed only one peak, which can be assigned to the M<sup>+</sup>-signal. Furthermore, elemental analysis of **1** is in good agreement with the calculated values, indicating that **1** is essentially pure.

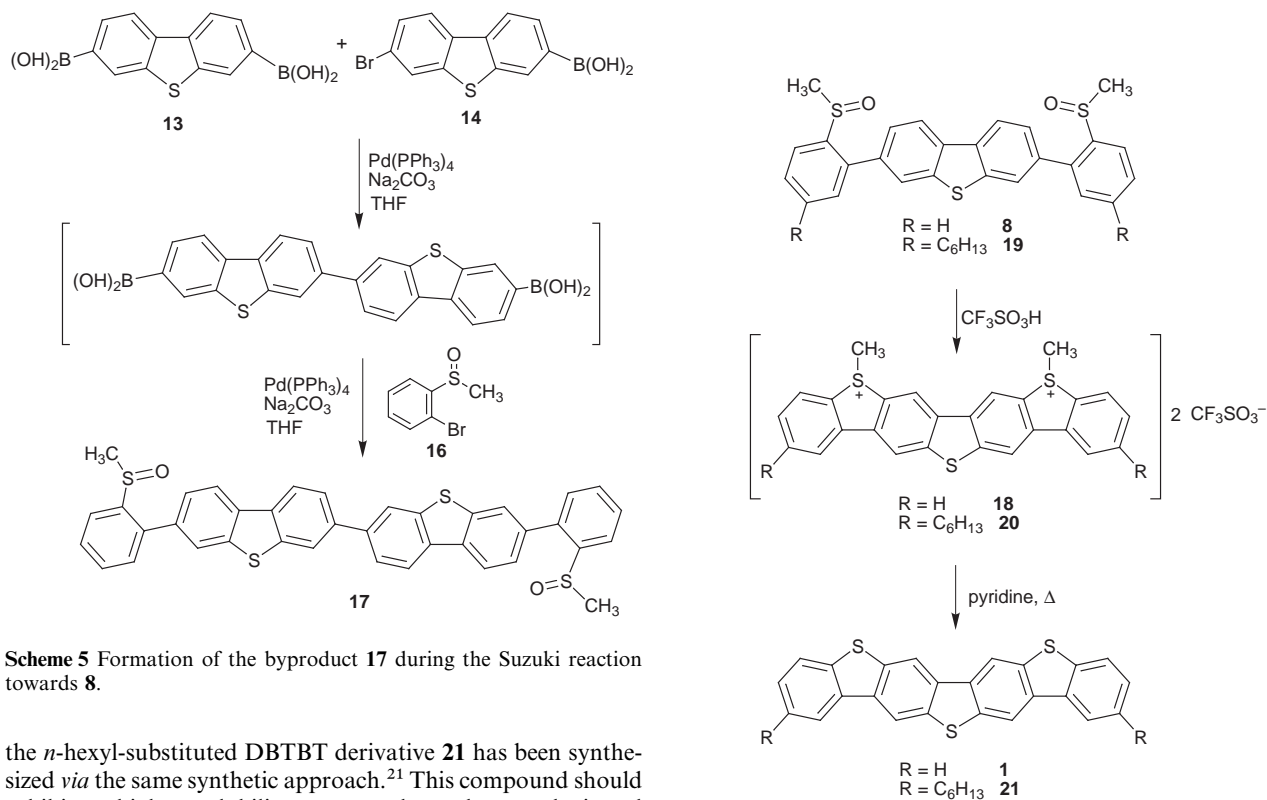
Considering the structure of the precursor molecule **8**, the reaction of the acid-induced coupling at different positions, namely *para* or *ortho* to the sulfide bridge, has to be taken into account. This would result in three possible regioisomers **1a-c** (Scheme 7). In the case of the intermolecular acid-induced coupling reactions of aromatic methyl sulfoxides *para*-substitution is exclusively observed.<sup>10-14</sup> The situation for the intramolecular coupling, on the other hand, might be completely different. As NMR spectroscopy on DBTBT **1** can not be performed, there is no possibility of specifying the exact distribution of the three isomers in the insoluble material. IR spectroscopy, however, reveals four different aromatic C-H out-of-plane vibrations at 724 (s), 755 (s), 814 (m) and 866 (s) cm<sup>-1</sup>. Whereas the first two peaks can be assigned to the four-adjacent-hydrogen vibration,<sup>20</sup> the peak at 814 cm<sup>-1</sup> is typical of the two-adjacent-hydrogen vibration and that at 866 cm<sup>-1</sup> of the single-hydrogen vibration. This IR spectrum clearly indicates that at least two of the three possible isomers are present in the DBTBT **1**. However, from the intensity of the peaks we can assume that the isomer **1a** is by far the dominant one. To get a better understanding of this problem,



**Scheme 3** Two possible precursor structures **7** and **8** for DBTBT **1**.



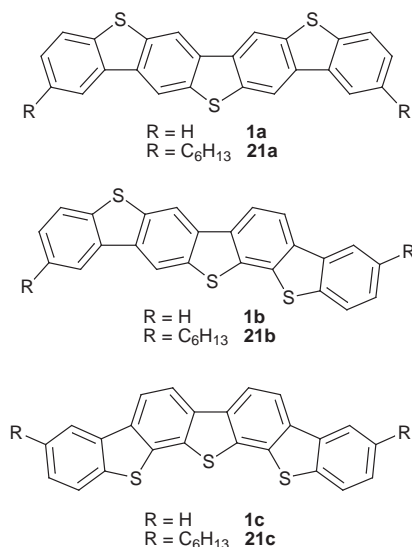
**Scheme 4** Synthetic route to the precursor **8** of DBTBT **1**.



**Scheme 5** Formation of the byproduct **17** during the Suzuki reaction towards **8**.

the *n*-hexyl-substituted DBTBT derivative **21** has been synthesized *via* the same synthetic approach.<sup>21</sup> This compound should exhibit a higher solubility compared to the unsubstituted DBTBT **1** due to the alkyl chains, which then might allow the recording of an NMR spectrum and hence a specification of the distribution of the isomers. The crude product obtained

**Scheme 6** Acid-induced cyclization reaction of the precursors **8** and **19** towards the target structure DBTBT **1** and the *n*-hexyl substituted system **21**.



**Scheme 7** Possible structures of the regioisomers **1a–c** and **21a–c**.

after acid-induced cyclization reaction and subsequent demethylation is indeed soluble in carbon disulfide and can be chromatographed on silica gel to obtain pure **21**. From the  $^1\text{H-NMR}$  spectrum (500 MHz,  $\text{CS}_2$  with drops of  $\text{CD}_2\text{Cl}_2$  for locking the field) of **21** we were able to distinguish between the three isomers and according to the signals of the aromatic protons, about 71% of the ‘desired’ isomer **21a** is contained in the mixture. Unfortunately, after one recrystallization either from carbon disulfide or from toluene the crystals were too insoluble in usual NMR solvents and carbon disulfide to obtain the composition of the isomers after recrystallization. In contrast to DBTBT **1**, IR spectroscopy on **21** can not provide any further information, as the substitution pattern of **21** does not allow a differentiation of the aromatic C–H out-of-plane vibrations for the three regioisomers. Since the alkyl substituents of the precursor **19** show a negligible electronic effect and no steric hindrance towards the reaction center during the acid-induced cyclization reaction, it is safe to assume that the distribution of the three regioisomers in **21** is comparable to that of the unsubstituted DBTBT **1**.

### 3. DBTBT field-effect transistor devices

Thin films of DBTBT **1** (30–100 nm) were deposited by vacuum sublimation under high vacuum ( $p < 10^{-6}$  mbar) at a rate of  $\approx 0.5\text{--}1 \text{ \AA s}^{-1}$  onto FET substrates consisting of highly doped  $n^+\text{-Si}$  wafers with a 230 nm dry thermal  $\text{SiO}_2$  gate oxide. The substrate temperature was varied between room temperature and  $150^\circ\text{C}$ . The best device performance was obtained for a substrate temperature of  $\approx 100^\circ\text{C}$ . Prior to the deposition the surface of the  $\text{SiO}_2$  substrate was treated with the silylating agent, hexamethyldisilazane (HMDS). This treatment makes the surface hydrophobic by replacing the natural hydrophilic hydroxy groups on the  $\text{SiO}_2$  surface with apolar methyl groups and results in improved charge carrier mobilities at the active interface. FET characteristics were measured with an HP4145B parameter analyzer under dry nitrogen atmosphere.

Fig. 1 shows the output (a) and transfer (b) characteristics of a typical DBTBT top-contact FET with Au S-D contacts. Transistor action is observed for negative gate voltages, *i.e.*, transport is due to positive hole carriers. The output characteristics are linear for small S-D voltage  $V_{\text{sd}}$  indicating that contact resistance effects do not limit the FET current. The transistors are normally-off, that is, they turn on at a negative gate voltage  $V_0 \approx -8 \text{ V}$ . At  $V_g = 0 \text{ V}$  the OFF current is only a few pA's and is limited by gate leakage. The ON–OFF

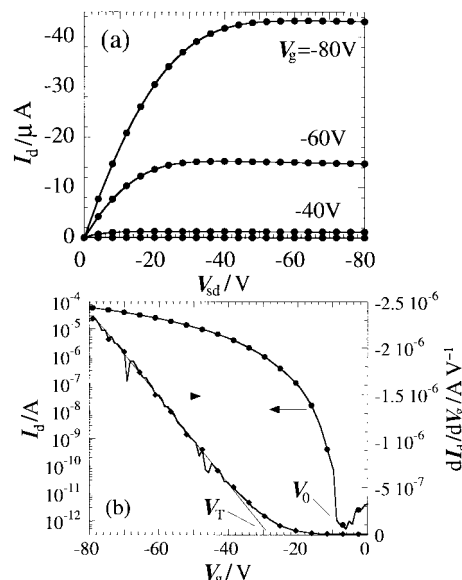


**Fig. 1** (a) Output characteristics of a top contact DBTBT FET. (b) Saturated transfer characteristics (left scale) and transconductance (right scale). From the slope of the transconductance in the saturation regime the mobility is determined (channel length  $L = 75 \mu\text{m}$ , channel width  $W = 1.5 \text{ mm}$ ,  $V_{\text{sd}} = -80 \text{ V}$ ).

current ratio exceeds  $10^6$  between  $V_g = 0$  and  $-40 \text{ V}$ . In many p-type, organic FETs a positive turn-voltage, that is, normally-on behavior, is observed.<sup>7</sup> This is often caused by unintentional extrinsic doping of the organic film.<sup>9</sup> A positive, reverse gate voltage is then required to deplete the bulk of the film. The negative turn-on voltage and the low OFF-current observed here give evidence for a low extrinsic doping level and conductivity  $\sigma$  of the film. From the output characteristics at  $V_g = 0 \text{ V}$   $\sigma$  is estimated to be  $< 10^{-9} \text{ S cm}^{-1}$ . Note that a negative  $V_0$  is expected from the negative work function difference between the  $n^+\text{-Si}$  gate and the Au S-D electrodes causing the flat-band voltage in the semiconductor to be  $< 0$ .  $V_0$  may also reflect interfacial band bending in the semiconductor due to a distribution of localized interface states (see below).

The field-effect mobility can be determined from the transconductance  $dI_d/dV_g$  in the saturation regime [eqn. (1)].<sup>22</sup>

$$\frac{dI_d}{dV_g} = \frac{C_i \cdot W}{L} \cdot \mu_{\text{FET}}^{\text{sat}}(V_g) \cdot (V_g - V_T) \quad (1)$$

Depending on the distribution of disorder-induced localized states below the charge transport level the field-effect mobility  $\mu_{\text{FET}}(V_g)$  may depend on the gate voltage, that is, the position of the Fermi level at the interface.<sup>2</sup> In this case the transconductance would be expected to exhibit a superlinear dependence on the gate voltage. The transconductance of DBTBT FETs increases linearly above a threshold voltage  $V_T = -28 \text{ V}$  indicating that above  $V_T$  the mobility is independent of the gate voltage. From the slope of the transconductance curve we extract  $\mu_{\text{FET}}^{\text{sat}} = 0.15 \pm 0.05 \text{ cm}^2 \text{ V}^{-1} \text{ s}^{-1}$ . Similar values are obtained from the transfer characteristics in the linear regime ( $V_{\text{sd}} \ll V_g$ ). This mobility is among the highest ones reported for polycrystalline oligomer FETs. It is similar to that of anthradithiophene (ADT)<sup>5</sup> and dihexylquaterthiophene.<sup>6</sup> Higher values have only been obtained for quasi single-crystalline films of pentacene<sup>7</sup> and bulk single-crystals of oligothiophenes.<sup>23</sup> The relatively high value of the threshold voltage  $V_T$  reflects the presence of localized interface states/traps that need to be filled before the mobility becomes gate-voltage independent.

The DBTBT films exhibit a high degree of structural order as is evident from  $\theta\text{-}2\theta$  X-ray diffraction measurements (Fig. 2). In a direction normal to the film plane only one

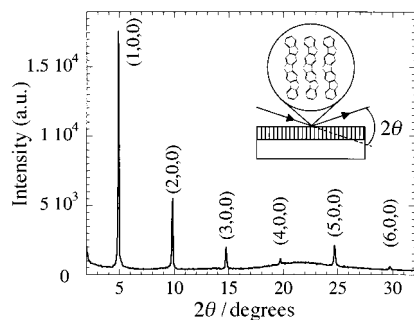


**Fig. 2** Cu K $\alpha$   $\theta$ - $2\theta$  XRD diffraction pattern of a thin DBTBT film. Only Bragg reflections normal to the substrate plane can be observed in this scattering geometry. The broad peak centered at  $2\theta \approx 22^\circ$  is due to scattering from the amorphous glass substrate. The reflections from the thin polycrystalline film belong to a single set of lattice planes indicating a preferential orientation of the grains.

family of lattice reflections is observed. This shows that the polycrystalline grains of the film have a single preferential orientation. The Bragg reflections belong to a periodicity of  $18.0 \pm 0.2 \text{ \AA}$  which is close to the length of the DBTBT molecule. Although the single-crystal structure of DBTBT is not known, the XRD pattern suggests that the molecules are oriented with their long axis normal to the film. This orientation is similar to that of most other thiophene oligomers and gives rise to high mobilities due to intermolecular  $\pi$ - $\pi$  stacking in the plane of the film.

#### 4. Effect of different regioisomers on FET performance

The high mobilities reported above were obtained when the substrate shutter during the evaporation was opened after a substantial fraction of the freshly loaded material in the crucible had already sublimed. If the shutter was opened immediately after the evaporation rates had stabilized, FETs with degraded performance were obtained. For these devices a superlinear dependence of the transconductance on the gate voltage is observed (Fig. 3) in contrast to the linear behavior discussed above (Fig. 1b). This indicates that the mobility depends on the gate voltage [eqn. (1)].<sup>2</sup> The mobility is lower by typically a factor of 5–10 than in the high-mobility devices discussed above. The turn-on voltage is shifted to  $V_0 \approx -19 \text{ V}$ . The ON-OFF characteristics are less steep, the subthreshold slope is typically  $4 \text{ V decade}^{-1}$  compared to  $1 \text{ V decade}^{-1}$  in the high-mobility FETs. The subthreshold slope is a measure of how fast the Fermi level at the interface is moved by the applied gate voltage from its flat band position towards the charge transport level. A high value reflects a high density of localized electronic defect states in the semiconductor at the interface. These observations suggest that DBTBT films grown from the first sublimation fractions of the as-synthesized

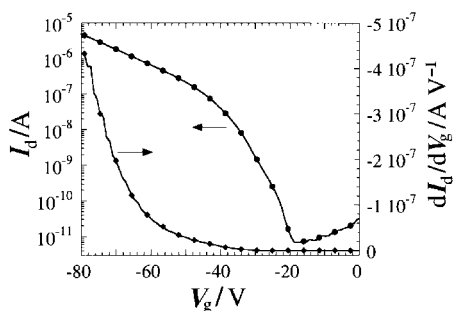


**Fig. 3** Saturated transfer characteristics and transconductance of a top-contact DBTBT FET grown from the first sublimation fractions of as-synthesized DBTBT ( $L = 154 \text{ \mu m}$ ,  $W = 1.5 \text{ mm}$ ,  $V_{sd} = -80 \text{ V}$ ).

material are more disordered. In XRD diffraction measurements on such samples only the ( $h00$ ) reflections with  $h = 1, 2, 3$  can be resolved with rapidly decreasing intensities for increasing  $h$ .

This suggests that the as-synthesized material contains different volume fractions. Since the elemental analysis and mass spectrometry exclude the presence of significant amounts of chemical impurities, the most plausible explanation is the presence of different regioisomers of DBTBT. As discussed above three regioisomers **1a–c** have indeed been identified by infrared spectroscopy of DBTBT and NMR spectroscopy of di-alkyl substituted DBTBT. When the substrate shutter is opened after a substantial amount of the crucible material has already sublimed, volume fractions with slightly lower sublimation temperature than the main fraction have been removed, and the material deposited onto the substrate is effectively purified. In practice, this separation of the different fractions was often found to be difficult due to the rather small differences of sublimation temperature.

This interpretation is confirmed by optical absorption spectroscopy on thin films (Fig. 4). On samples with mobilities  $> 0.1 \text{ cm}^2 (\text{Vs})^{-1}$  a strong absorption peak is observed at  $E_1 = 2.99 \text{ eV}$  with vibronic replica at  $E_2 = 3.16 \text{ eV}$ . In contrast, samples with mobilities of the order of  $10^{-2} \text{ cm}^2 (\text{Vs})^{-1}$  exhibit a strong transition at  $E_1' = 3.14 \text{ eV}$  with vibronic replica at  $E_2' = 3.30 \text{ eV}$ . A shoulder coinciding approximately with the energy of the  $E_1$  transition of the high mobility sample is also clearly resolved. This spectrum can be interpreted as a superposition of two components. The first component has a spectrum close to that of the high mobility sample. The second component has a similar shape, but is shifted to higher energies by  $\approx 0.14 \text{ eV}$ . The relative weights of the two components have been found to vary with the deposition procedure. The lower the content of material in the film from the early stages of sublimation the stronger is the transition  $E_1$  compared to  $E_1'$ . These observations are consistent with the existence of different regioisomers. The isomer in which the first allowed optical transition in the solid state occurs at the lowest energy exhibits the highest mobility. This is believed to be the isomer **1a**, which is the dominant volume fraction.

A detailed interpretation of the solid-state optical spectra in terms of the fundamental  $\pi$ - $\pi^*$  absorption of the isolated molecules and intermolecular interaction effects in the solid state cannot be given at present, since the spectra of isolated molecules in solution could not be obtained. Due to the very low solubility of DBTBT aggregation effects cannot be avoided even in dilute solutions. However, it is worth pointing out that the first optical transition of DBTBT in the solid state occurs at significantly lower energy than that of corresponding *para*-phenylene oligomers without thiophene bridges.<sup>24</sup>

#### 5. Conclusions

We have shown that the acid-induced cyclization reaction of aromatic methyl sulfoxides is a novel tool for the formation

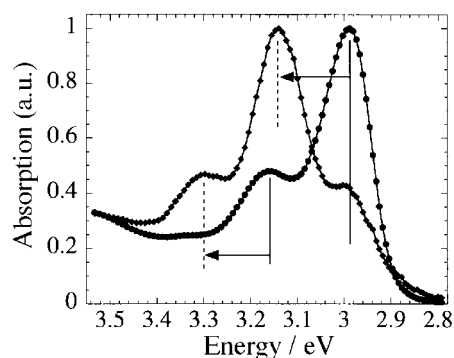


**Fig. 4** Optical absorption spectra of DBTBT films exhibiting high (circles, Fig. 1) and low FET mobility (diamonds, Fig. 3).

of dibenzothiophene-based compounds in high yield. Through this technique it was for the first time possible to synthesize DBTBT **1**. This intramolecular coupling reaction is not regioselective compared to its intermolecular analogue and gives a mixture of different regio-isomers, however, with the exclusively *para*-coupled isomer as the dominating species. FET devices in which the DBTBT film contains a mixture of regio-isomers only exhibit field-effect mobilities  $<0.03 \text{ cm}^2 \text{ V}^{-1} \text{ s}^{-1}$ . However, if DBTBT is purified by vacuum sublimation, mobilities up to  $0.15 \text{ cm}^2 \text{ V}^{-1} \text{ s}^{-1}$  and ON-OFF current ratios  $>10^6$  have been obtained. The mobility is among the highest ones reported for polycrystalline organic FETs. This makes DBTBT a promising material for organic FETs and, possibly, a suitable building block for high-mobility conjugated polymers. These results provide further insight into the electrical properties of long, fused-ring conjugated molecules and warrant the complex and difficult synthesis of DBTBT.

It is not known to what extent the mobility value of  $0.15 \text{ cm}^2 \text{ V}^{-1} \text{ s}^{-1}$  is still limited by the polycrystalline grain morphology of the DBTBT films and/or residual isomer impurities. Our results show that to obtain high mobilities in fused-ring, thiophene-based oligomers a rigorous purification to separate different regioisomers is crucially important.

## 6. Experimental

### General methods

Commercial reagents were used without further purification. Solvents were purified, dried and degassed following standard procedures.  $^1\text{H}$  and  $^{13}\text{C}$  NMR spectral data were obtained on a Varian Gemini 200 (200 MHz), a Bruker DRX-250 (250 MHz) and a Bruker AMX 500 (500 MHz) spectrometer. IR spectra were measured on a Nicolet 320 FT-IR spectrometer. FD-mass spectra were obtained from a ZAB2-SE-FPD instrument. The UV-VIS spectra were recorded on a Perkin-Elmer Lambda 9 spectrophotometer. Thermal analysis was carried out using a Mettler DSC 30 differential scanning calorimeter.

### Synthesis

**2-(Methylsulfanyl)biphenyl (3)**. 2-Bromobiphenyl (**2**) (1 g, 4.3 mmol) was dissolved in dry THF (15 ml) and cooled to  $-78^\circ\text{C}$ . *n*-Butyllithium solution (1.6 M in hexane, 2.7 ml, 4.3 mmol) was added dropwise at low temperature. After the addition was complete the mixture was stirred for an additional hour, while a precipitate formed. Dimethyl disulfide (0.36 g, 4.3 mmol) was added dropwise. The cooling bath was removed and the solution was stirred at room temperature for 2 h. Water was added and the mixture was extracted with dichloromethane. The solvent was evaporated under reduced pressure. Crystallisation of the crude product from methanol afforded 0.66 g (77%) of **3** as colorless plates. mp:  $41\text{--}43^\circ\text{C}$ .  $^1\text{H-NMR}$  (250 MHz,  $\text{CD}_2\text{Cl}_2$ ):  $\delta=7.51\text{--}7.34$  (m, 7H, 7 Ar-H),  $7.29\text{--}7.26$  (m, 2H, 2Ar-H), 2.42 (s, 3H, S- $\text{CH}_3$ ).  $^{13}\text{C-NMR}$  (62.5 MHz,  $\text{CD}_2\text{Cl}_2$ ):  $\delta=141.07, 140.97, 137.55, 130.29, 129.69, 128.42, 128.31, 127.80, 125.45, 124.98, 16.06$ . FD-MS (8 kV):  $m/z=200.3$  (100%) [ $\text{M}^+$ ].

**2-(Methylsulfinyl)biphenyl (4)**. 2-(Methylsulfinyl)biphenyl (**3**) (0.5 g, 2.5 mmol) was dissolved in glacial acetic acid (10 ml). Hydrogen peroxide (35%, 0.25 g) dissolved in glacial acetic acid (10 ml) was added dropwise to the solution. The mixture was allowed to stir at room temperature for 12 h. The acetic acid was removed by evaporation under vacuum and the crude product was crystallized from cyclohexane, affording 0.48 g (90%) of **4** as colorless needles. mp:  $92\text{--}94^\circ\text{C}$ .  $^1\text{H-NMR}$  (250 MHz,  $\text{CD}_2\text{Cl}_2$ ):  $\delta=8.08$  (dd, 1H,  $^3J=7.53 \text{ Hz}$ ,  $^4J=1.60 \text{ Hz}$ , 1 Ar-H), 7.62 (dt, 1H,  $^3J=7.53 \text{ Hz}$ ,  $^4J=1.57 \text{ Hz}$ , 1 Ar-H), 7.55 (dt, 1H,  $^3J=7.54 \text{ Hz}$ ,  $^4J=1.56 \text{ Hz}$ , 1 Ar-H),

7.47–7.30 (m, 6H, 6 Ar-H), 2.33 (s, 3H, SO- $\text{CH}_3$ ).  $^{13}\text{C-NMR}$  (62.5 MHz,  $\text{CD}_2\text{Cl}_2$ ):  $\delta=144.77, 139.80, 138.34, 130.87, 130.64, 129.50, 129.02, 128.97, 128.54, 123.52$ . FD-MS (8 kV):  $m/z=216.05$  (100%) [ $\text{M}^+$ ].

**Dibenzothiophene (6)**. 2-(Methylsulfinyl)biphenyl (**4**) (200 mg, 0.9 mmol) was added to trifluoromethanesulfonic acid (4.5 ml). The solution was stirred at room temperature for 48 h and then poured slowly into a water-pyridine mixture (60 ml, 5:1). Demethylation was achieved by heating the mixture to reflux for 10 min. Upon cooling **6** crystallizes as colorless plates in 90% yield.

**3,7-Dibromodibenzothiophene dioxide (11)**. To the stirred solution of dibenzothiophene dioxide (**10**) (8.64 g, 40 mmol) in sulfuric acid (300 ml), dibromocyanuric acid powder (13.2 g, 46 mmol) was added in one portion. The mixture was stirred vigorously at room temperature for 12 h. The milky yellow suspension was poured onto ice and stood overnight. A white solid was collected by decantation and suction filtration, followed by washing with water, 5% KOH solution, then water successively. Crystallisation of the solid from chlorobenzene yielded 8.5 g (57%) colorless needles of **11**. mp:  $288\text{--}290^\circ\text{C}$ .  $^1\text{H-NMR}$  (200 MHz, DMSO):  $\delta=8.34$  (d, 2H,  $^3J=8.36 \text{ Hz}$ , 2 Ar-H), 8.16 (d, 2H,  $^3J=8.36 \text{ Hz}$ , 2 Ar-H), 8.02 (dd, 2H,  $^3J=8.34 \text{ Hz}$ ,  $^4J=1.70 \text{ Hz}$ , 2 Ar-H).  $^{13}\text{C-NMR}$  (50 MHz, DMSO):  $\delta=138.63, 137.86, 129.55, 125.38, 125.12, 124.35$ . FD-MS (8 kV):  $m/z=373.7$  (100%) [ $\text{M}^+$ ].

**3,7-Dibromodibenzothiophene (12)**. 3,7-Dibromodibenzothiophene dioxide (**11**) (4.05 g, 10.8 mmol) was suspended in dry diethyl ether (80 ml). Lithium aluminium hydride (2.0 g) was added slowly at room temperature to maintain a moderate reflux. When the addition was complete, the mixture was stirred and refluxed for an additional 2 h. Water was added very carefully to destroy excess  $\text{LiAlH}_4$  and then concentrated hydrochloric acid (10 ml) was added. Diethyl ether was removed by evaporation and the resulting mixture was filtered to obtain a colorless solid. Crystallisation of the solid from chloroform afforded 2.19 g (59%) of **12** as colorless needles. mp:  $169\text{--}170^\circ\text{C}$ .  $^1\text{H-NMR}$  (200 MHz,  $\text{CDCl}_3$ ):  $\delta=7.95$  (s, 2H, 2 Ar-H), 7.91 (d, 2H,  $^3J=8.42 \text{ Hz}$ , 2 Ar-H), 7.54 (d, 2H,  $^3J=8.42 \text{ Hz}$ , 2 Ar-H).  $^{13}\text{C-NMR}$  (50 MHz,  $\text{CDCl}_3$ ):  $\delta=140.91, 133.72, 128.16, 125.49, 122.65, 120.84$ . FD-MS (8 kV):  $m/z=341.6$  (100%) [ $\text{M}^+$ ].

**Dibenzothiophene-3,7-diboronic acid (13)**. 3,7-Dibromodibenzothiophene (**12**) (3.85 g, 11.25 mmol) was dissolved in dry THF (200 ml) and the solution was cooled to  $-78^\circ\text{C}$ . *tert*-Butyllithium solution (1.5 M in pentane, 15 ml, 22.5 mmol) was added dropwise at low temperature. Cooling and stirring were maintained for an additional 5 h. Triisopropyl borate (15 ml, 65 mmol) was added to the milky colorless to light yellow slurry in one portion at  $-78^\circ\text{C}$  and the mixture was stirred for 0.5 h and then for 1 h at room temperature. The mixture was cooled again to  $-78^\circ\text{C}$  and 1 M hydrochloric acid (100 ml) was added. The cooling bath was removed after the addition and the mixture was stirred at room temperature for 1 h. THF was removed under reduced pressure and a white solid was collected by suction filtration. The solid was dissolved in 5% KOH solution (50 ml) and the solution was filtered through Celite to remove any insoluble impurities. The filtrate was acidified with 1 M hydrochloric acid and 2.85 g (93% based on **13**) of a white solid was obtained by suction filtration and drying under vacuum. This solid contained 3-bromodibenzothiophene-7-boronic acid (**14**) as a byproduct, which could not be separated from **13**. Therefore it was impossible to determine the exact yield for this reaction.  $^1\text{H-NMR}$  (200 MHz, DMSO):  $\delta=8.39$  (s, 2H, 2 Ar-H), 8.35 (d, 2H,

$^3J=8.06$  Hz, 2 Ar-H), 8.20 (s, 4H, 2 B-(OH)<sub>2</sub>), 7.93 (d, 2H,  $^3J=8.06$  Hz, 2 Ar-H).

**2-Bromo(methylsulfinyl)benzene (16).** 2-Bromothioanisole (**15**) (3.3 g, 16.25 mmol) was dissolved in glacial acetic acid and cooled with an ice-bath till the solvent was about to freeze. Hydrogen peroxide (35%, 1.81 g) was added slowly. The cooling bath was removed and the mixture was stirred at room temperature for 12 h. Acetic acid was removed by vacuum evaporation and water (50 ml) was added to the residue. The precipitated oil was taken up with dichloromethane, the solution washed with saturated NaHCO<sub>3</sub> solution and dried over MgSO<sub>4</sub>. Evaporation of the solvent yielded 3.5 g (98%) of **16** as a viscous colorless oil. <sup>1</sup>H-NMR (200 MHz, CDCl<sub>3</sub>):  $\delta=7.96$  (m, 1H, 1 Ar-H), 7.59 (m, 2H, 2 Ar-H), 7.38 (m, 1H, 2 Ar-H), 2.82 (s, 3H, S-CH<sub>3</sub>). <sup>13</sup>C-NMR (50 MHz, CDCl<sub>3</sub>):  $\delta=145.25, 132.63, 131.98, 128.43, 125.38, 117.81, 41.69$ . FD-MS (8 kV):  $m/z=218.9$  (100%) [ $M^+$ ].

**3,7-Bis[2-(methylsulfinyl)phenyl]dibenzothiophene (8).** To the stirred solution of sulfoxide **16** (2.63 g, 12 mmol) in freshly distilled THF (150 ml), Pd(PPh<sub>3</sub>)<sub>4</sub> (416 mg, 0.36 mmol) was added in one portion under argon. The mixture was stirred for 10 min, then diboronic acid **13** (1.36 g, 5 mmol) and 2 M Na<sub>2</sub>CO<sub>3</sub> solution (15 ml) were added. The flask was covered with aluminium foil and the mixture was heated to reflux and stirred vigorously for 20 h. THF was evaporated followed by decantation of the upper water phase to obtain a greenish-yellow oily residue. The soluble part of the residue was chromatographed (silica gel, EtOAc–MeOH (9:1)) to get a white solid of **8** (1.81 g, 51%). From a second fraction 0.25 g of byproduct **17** were isolated as a white solid. The formation of the latter compound **17** is described in Scheme 5. Mp of both compounds >300 °C. Spectral data of **8**: <sup>1</sup>H-NMR (250 MHz, CDCl<sub>3</sub>):  $\delta=8.24$  (d, 2H,  $^3J=6.52$  Hz, 2 Ar-H), 8.15 (dd, 2H,  $^3J=6.54$  Hz,  $^4J=1.26$  Hz, 2 Ar-H), 7.88 (d, 2H,  $^4J=1.26$  Hz, 2 Ar-H), 7.65 (dt, 2H,  $^3J=6.54$  Hz,  $^4J=1.26$  Hz, 2 Ar-H), 7.57 (dt, 2H,  $^3J=6.54$  Hz,  $^4J=1.26$  Hz, 2 Ar-H), 7.50 (dd, 2H,  $^3J=6.54$  Hz,  $^4J=1.26$  Hz, 2 Ar-H), 2.36 (s, 6H, SO-CH<sub>3</sub>). <sup>13</sup>C-NMR (62.5 MHz, CDCl<sub>3</sub>):  $\delta=144.00, 140.33, 138.78, 136.83, 134.75, 130.82, 130.51, 129.09, 125.89, 123.53, 123.32, 122.02, 41.70$ . FD-MS (8 kV):  $m/z=460.5$  (100%) [ $M^+$ ].

Spectral data of **17**: <sup>1</sup>H-NMR (250 MHz, CDCl<sub>3</sub>):  $\delta=8.24$  (t, 4H,  $^3J=5.78$  Hz, 4 Ar-H), 8.15 (dd, 4H,  $^3J=5.78$  Hz,  $^4J=1.26$  Hz, 4 Ar-H), 7.86 (d, 2H,  $^4J=1.26$  Hz, 2 Ar-H), 7.80 (dd, 2H,  $^3J=5.78$  Hz,  $^4J=1.26$  Hz, 2 Ar-H), 7.65 (dt, 2H,  $^3J=5.78$  Hz,  $^4J=1.26$  Hz, 2 Ar-H), 7.56 (dt, 2H,  $^3J=5.78$  Hz,  $^4J=1.26$  Hz, 2 Ar-H), 7.47 (dd, 2H,  $^3J=5.78$  Hz,  $^4J=1.26$  Hz, 2 Ar-H), 7.39 (dd, 2H,  $^3J=5.78$  Hz,  $^4J=1.26$  Hz, 2 Ar-H) 2.37 (s, 6H, SO-CH<sub>3</sub>). <sup>13</sup>C-NMR (62.5 MHz, CDCl<sub>3</sub>):  $\delta=143.93, 140.64, 140.30, 139.75, 138.92, 136.42, 135.03, 134.21, 130.80, 130.53, 129.01, 125.72, 124.32, 123.51, 123.26, 122.14, 121.86, 121.39, 41.68$ . FD-MS (8 kV):  $m/z=642.1$  (100%) [ $M^+$ ].

**Dibenzo[*b,b'*]thieno[2,3-*f*:5,4-*f'*]bis[1]benzothiophene (DBTBT, **1**).** A 10 ml round bottomed flask was filled with 3,7-bis[2-(methylsulfinyl)phenyl]dibenzothiophene (**8**) (270 mg, 0.59 mmol) and trifluoromethanesulfonic acid (3 ml). The mixture was stirred for 12 h at room temperature to give a dark green solution, which was then poured into ice–water

(100 ml). The yellow precipitate was collected by suction filtration and washed with a large amount of methanol. The structure of this compound, which was insoluble in ordinary organic solvents, was assumed to be **18**. Demethylation of the solid was achieved by refluxing in pyridine (20 ml) for 12 h. When the suspension was cooled to room temperature, a large volume of acetone was added. DBTBT **1** was thus obtained by suction filtration and crystallisation from boiling quinoline as pale yellow plates (210 mg, 86% related to **8**). mp: 299.6 °C (determined by differential scanning calorimetry (DSC)). FD-MS:  $m/z=396.0$  (100%) [ $M^+$ ]. Anal. Calc. for C<sub>24</sub>H<sub>12</sub>S<sub>3</sub>: C 72.69, H 3.05; found: C 72.63, H 3.19%.

## Acknowledgements

Financial support from the British Royal Society (URF) and the Engineering and Physical Sciences Research Council is gratefully acknowledged. JL thanks the Fonds der Chemischen Industrie for a stipend.

## References

- 1 C. J. Drury, C. M. J. Mutsaers, C. M. Hart, M. Matters and D. M. de Leeuw, *Appl. Phys. Lett.*, 1998, **73**, 108.
- 2 H. Sirringhaus, N. Tessler and R. H. Friend, *Science*, 1998, **280**, 1741.
- 3 H. E. Katz, *J. Mater. Chem.*, 1997, **7**, 369.
- 4 F. Garnier, R. Hajlaoui, A. Yassar and P. Srivastava, *Science*, 1994, **265**, 1684.
- 5 J. G. Laquindanum, H. E. Katz and A. J. Lovinger, *J. Am. Chem. Soc.*, 1998, **120**, 664.
- 6 H. E. Katz, A. J. Lovinger and J. G. Laquindanum, *Chem. Mater.*, 1998, **10**, 457.
- 7 Y. Y. Lin, D. J. Gundlach, S. F. Nelson and T. N. Jackson, *IEEE Trans. Electron. Devices*, 1997, **44**, 1325.
- 8 J. G. Laquindanum, H. E. Katz, A. J. Lovinger and A. Dodabalapur, *Adv. Mater.*, 1997, **9**, 36.
- 9 H. Sirringhaus, R. H. Friend, X. C. Li, S. C. Moratti, A. B. Holmes and N. Feeder, *Appl. Phys. Lett.*, 1997, **71**, 3871.
- 10 K. Yamamoto, E. Shouji, H. Nishide and E. Tsuchida, *J. Am. Chem. Soc.*, 1993, **115**, 5819.
- 11 E. Tsuchida, E. Shouji and K. Yamamoto, *Macromolecules*, 1993, **26**, 7144.
- 12 L. Wang, T. Soczka-Guth, E. Havinga and K. Müllen, *Angew. Chem., Int. Ed. Engl.*, 1996, **35**, 1495.
- 13 J. Leuninger, C. Wang, T. Soczka-Guth, V. Enkelmann, T. Pakula and K. Müllen, *Macromolecules*, 1998, **31**, 7120.
- 14 J. Leuninger, J. Uebe, J. Salbeck, L. Gherghel, C. Wang and K. Müllen, *Synth. Met.*, 1999, in the press.
- 15 R. M. Acheson and J. K. Stubbs, *J. Chem. Soc., Perkin Trans. 1*, 1972, **1**, 899.
- 16 N. M. Cullinane and C. G. Davies, *J. Chem. Soc.*, 1936, 1435.
- 17 W. Gottardi, *Monatsh. Chem.*, 1968, **98**, 507.
- 18 R. Gerdil and E. A. C. Lucken, *J. Am. Chem. Soc.*, 1965, **87**, 213.
- 19 N. Miyaura and A. Suzuki, *Chem. Rev.*, 1995, **95**, 2457.
- 20 S. E. Wiberly and R. D. Gonzalez, *Appl. Spectrosc.*, 1961, **15**, 174.
- 21 J. Leuninger, PhD Thesis, Johannes Gutenberg-Universität, Mainz (1999).
- 22 M. S. Shur, M. Hack and J. G. Shaw, *J. Appl. Phys.*, 1989, **66**, 3371.
- 23 J. H. Schön, C. Kloc, R. A. Laudise and B. Batlogg, *Phys. Rev. B*, 1998, **58**, 12952.
- 24 J. Grimme, M. Kreyenschmidt, F. Uckert, K. Müllen and U. Scherf, *Adv. Mater.*, 1995, **7**, 292.

Paper 9/02679G